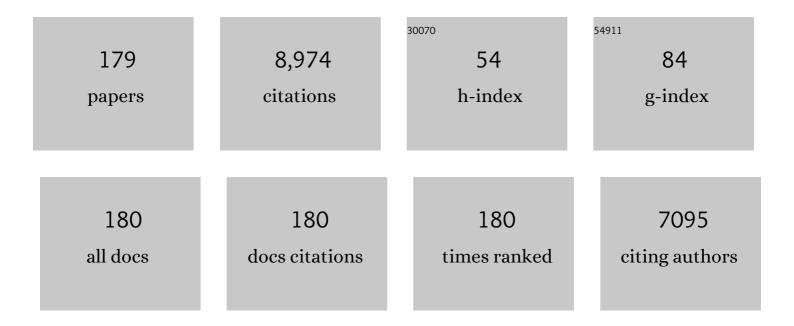
Chongxuan Liu

List of Publications by Year in descending order

Source: https://exaly.com/author-pdf/3439564/publications.pdf Version: 2024-02-01



Сноисхиля Ци

#	Article	IF	CITATIONS
1	Legacy Effects of Sorption Determine the Formation Efficiency of Mineral-Associated Soil Organic Matter. Environmental Science & Technology, 2022, 56, 2044-2053.	10.0	21
2	Formation, aggregation, and transport of NOM–Cr(<scp>iii</scp>) colloids in aquatic environments. Environmental Science: Nano, 2022, 9, 1133-1145.	4.3	10
3	Fast cost-effective synthesis of metal ions/biopolymer/silica composites by supramolecular hydrogels crosslink with superior tetracycline sorption performance. Chemosphere, 2022, 294, 133821.	8.2	5
4	Prediction of saturated hydraulic conductivity of sandy soil using Sauter mean diameter of soil particles. European Journal of Soil Science, 2022, 73, .	3.9	2
5	Effects of geochemical and hydrodynamic transiency on desorption and transport of As in heterogeneous systems. Science of the Total Environment, 2022, 835, 155381.	8.0	0
6	Microbial metabolism changes molecular compositions of riverine dissolved organic matter as regulated by temperature. Environmental Pollution, 2022, 306, 119416.	7.5	11
7	N-doped porous carbon spheres as metal-free electrocatalyst for oxygen reduction reaction. Journal of Materials Chemistry A, 2021, 9, 5751-5758.	10.3	46
8	Effects of flow-interruption on the bacteria transport behavior in porous media. Journal of Hydrology, 2021, 595, 125677.	5.4	7
9	Quantifying the multi-scale kinetic processes in soil environments: Frontiers and challenges. Fundamental Research, 2021, 1, 334-336.	3.3	2
10	Evaluation of a Data-Driven, Machine Learning Approach for Identifying Potential Candidates for Environmental Catalysts: From Database Development to Prediction. ACS ES&T Engineering, 2021, 1, 1246-1257.	7.6	8
11	The feedback interaction between biomass accumulation and heterogeneous flow in porous media: Effect of shear stresses. Journal of Hydrology, 2021, 597, 126083.	5.4	6
12	Watershed-scale water environmental capacity estimation assisted by machine learning. Journal of Hydrology, 2021, 597, 126310.	5.4	8
13	Chemodiversity of water-extractable organic matter in sediment columns of a polluted urban river in South China. Science of the Total Environment, 2021, 777, 146127.	8.0	32
14	Dynamics of dissolved organic matter and dissolved organic nitrogen during anaerobic/anoxic/oxic treatment processes. Bioresource Technology, 2021, 331, 125026.	9.6	30
15	Effects of chronic exposure of antibiotics on microbial community structure and functions in hyporheic zone sediments. Journal of Hazardous Materials, 2021, 416, 126141.	12.4	37
16	River restoration changes distributions of antibiotics, antibiotic resistance genes, and microbial community. Science of the Total Environment, 2021, 788, 147873.	8.0	23
17	Dynamic relationship between dissolved organic matter and soluble microbial products during wastewater treatment. Journal of Cleaner Production, 2021, 317, 128448.	9.3	27
18	Interfacial photoreactions of Cr(VI) and oxalate on lepidocrocite surface under oxic and acidic conditions: Reaction mechanism and potential implications for contaminant degradation in surface waters. Chemical Geology, 2021, 583, 120481.	3.3	16

#	Article	IF	CITATIONS
19	Enhanced sequestration of tetracycline by Mn(II) encapsulated mesoporous silica nanoparticles: Synergistic sorption and mechanism. Chemosphere, 2021, 284, 131334.	8.2	15
20	Watershed-scale distributions of heavy metals in the hyporheic zones of a heavily polluted Maozhou River watershed, southern China. Chemosphere, 2020, 239, 124773.	8.2	15
21	Coupled dynamics of As-containing ferrihydrite transformation and As desorption/re-adsorption in presence of sulfide. Journal of Hazardous Materials, 2020, 384, 121287.	12.4	25
22	Immobilization of Cr(VI) on engineered silicate nanoparticles: Microscopic mechanisms and site energy distribution. Journal of Hazardous Materials, 2020, 383, 121145.	12.4	18
23	Aerobic composting as an effective cow manure management strategy for reducing the dissemination of antibiotic resistance genes: An integrated meta-omics study. Journal of Hazardous Materials, 2020, 386, 121895.	12.4	68
24	Differential responses of stream water and bed sediment microbial communities to watershed degradation. Environment International, 2020, 134, 105198.	10.0	46
25	Impact of Physico-Chemical Heterogeneity on Arsenic Sorption and Reactive Transport under Water Extraction. Environmental Science & amp; Technology, 2020, 54, 14974-14983.	10.0	8
26	Heavy Metal Accumulation and Release Risks in Sediments from Groundwater–River Water Interaction Zones in a Contaminated River under Restoration. ACS Earth and Space Chemistry, 2020, 4, 2391-2402.	2.7	11
27	Tuning the Biodegradability of Chitosan Membranes: Characterization and Conceptual Design. ACS Sustainable Chemistry and Engineering, 2020, 8, 14484-14492.	6.7	19
28	Reduced NOM triggered rapid Cr(VI) reduction and formation of NOM-Cr(III) colloids in anoxic environments. Water Research, 2020, 181, 115923.	11.3	56
29	Role of clay-associated humic substances in catalyzing bioreduction of structural Fe(III) in nontronite by Shewanella putrefaciens CN32. Science of the Total Environment, 2020, 741, 140213.	8.0	19
30	Conduction Band of Hematite Can Mediate Cytochrome Reduction by Fe(II) under Dark and Anoxic Conditions. Environmental Science & Technology, 2020, 54, 4810-4819.	10.0	52
31	Contamination profile of antibiotic resistance genes in ground water in comparison with surface water. Science of the Total Environment, 2020, 715, 136975.	8.0	73
32	The scaling of mineral dissolution rates under complex flow conditions. Geochimica Et Cosmochimica Acta, 2020, 274, 63-78.	3.9	3
33	Chemodiversity of Soil Dissolved Organic Matter. Environmental Science & Technology, 2020, 54, 6174-6184.	10.0	133
34	Nitrate bioreduction dynamics in hyporheic zone sediments under cyclic changes of chemical compositions. Journal of Hydrology, 2020, 585, 124836.	5.4	3
35	Contamination profiles and health risks of PFASs in groundwater of the Maozhou River basin. Environmental Pollution, 2020, 260, 113996.	7.5	21
36	Profiling microbial communities in a watershed undergoing intensive anthropogenic activities. Science of the Total Environment, 2019, 647, 1137-1147.	8.0	52

#	Article	IF	CITATIONS
37	Coupled Kinetics Model for Microbially Mediated Arsenic Reduction and Adsorption/Desorption on Iron Oxides: Role of Arsenic Desorption Induced by Microbes. Environmental Science & Technology, 2019, 53, 8892-8902.	10.0	30
38	Transport and retention of Shewanella oneidensis strain MR1 in water-saturated porous media with different grain-surface properties. Chemosphere, 2019, 233, 57-66.	8.2	11
39	Groundwater Impacts of Radioactive Wastes and Associated Environmental Modeling Assessment. , 2019, , 101-111.		1
40	Elucidating the Role of Sulfide on the Stability of Ferrihydrite Colloids under Anoxic Conditions. Environmental Science & Technology, 2019, 53, 4173-4184.	10.0	31
41	Iron Redox Chemistry and Its Environmental Impact: A Virtual Special Issue. ACS Earth and Space Chemistry, 2019, 3, 2374-2375.	2.7	5
42	Compositional changes of dissolved organic carbon during its dynamic desorption from hyporheic zone sediments. Science of the Total Environment, 2019, 658, 16-23.	8.0	40
43	Formation and stability of NOM-Mn(III) colloids in aquatic environments. Water Research, 2019, 149, 190-201.	11.3	64
44	Effect of ion exchange on the rate of aerobic microbial oxidation of ammonium in hyporheic zone sediments. Environmental Science and Pollution Research, 2018, 25, 8880-8887.	5.3	7
45	A Generalized-Rate Model for Describing and Scaling Redox Kinetics in Sediments Containing Variable Redox-Reactive Materials. Environmental Science & Technology, 2018, 52, 5268-5276.	10.0	3
46	Characterization of PM10 surrounding a cement plant with integrated facilities for co-processing of hazardous wastes. Journal of Cleaner Production, 2018, 186, 831-839.	9.3	18
47	Direct thermal drying of sludge using flue gas and its environmental benefits. Drying Technology, 2018, 36, 1006-1016.	3.1	10
48	Organic carbon sources and controlling processes on aquifer arsenic cycling in the Jianghan Plain, central China. Chemosphere, 2018, 208, 773-781.	8.2	20
49	Algae explosive growth mechanism enabling weather-like forecast of harmful algal blooms. Scientific Reports, 2018, 8, 9923.	3.3	17
50	A moisture function of soil heterotrophic respiration that incorporates microscale processes. Nature Communications, 2018, 9, 2562.	12.8	124
51	Microscale water distribution and its effects on organic carbon decomposition in unsaturated soils. Science of the Total Environment, 2018, 644, 1036-1043.	8.0	12
52	Uranium (VI) transport in saturated heterogeneous media: Influence of kaolinite and humic acid. Environmental Pollution, 2018, 240, 219-226.	7.5	49
53	Modelâ€Based Analysis of the Effects of Damâ€Induced River Water and Groundwater Interactions on Hydroâ€Biogeochemical Transformation of Redox Sensitive Contaminants in a Hyporheic Zone. Water Resources Research, 2018, 54, 5973-5985.	4.2	27
54	Identification of Hydrobiogeochemical Processes Controlling Seasonal Variations in Arsenic Concentrations Within a Riverbank Aquifer at Jianghan Plain, China. Water Resources Research, 2018, 54, 4294-4308.	4.2	21

#	Article	IF	CITATIONS
55	Groundwater Impacts of Radioactive Wastes and Associated Environmental Modeling Assessment. , 2018, , 1-12.		0
56	Effect of Water Chemistry and Hydrodynamics on Nitrogen Transformation Activity and Microbial Community Functional Potential in Hyporheic Zone Sediment Columns. Environmental Science & Technology, 2017, 51, 4877-4886.	10.0	79
57	Targeted quantification of functional enzyme dynamics in environmental samples for microbially mediated biogeochemical processes. Environmental Microbiology Reports, 2017, 9, 512-521.	2.4	16
58	Welcome to <i>ACS Earth and Space Chemistry</i> . ACS Earth and Space Chemistry, 2017, 1, 1-2.	2.7	0
59	Coupled Hydro-Biogeochemical Processes Controlling Cr Reductive Immobilization in Columbia River Hyporheic Zone. Environmental Science & Technology, 2017, 51, 1508-1517.	10.0	44
60	Redox transformation and reductive immobilization of Cr(VI) in the Columbia River hyporheic zone sediments. Journal of Hydrology, 2017, 555, 278-287.	5.4	18
61	Chlorobenzene Release During Thermal Drying of Sludge: Mechanism and Source. Water, Air, and Soil Pollution, 2017, 228, 1.	2.4	6
62	Functional Enzyme-Based Approach for Linking Microbial Community Functions with Biogeochemical Process Kinetics. Environmental Science & Technology, 2017, 51, 11848-11857.	10.0	27
63	Arsenic speciation in aquifer sediment under varying groundwater regime and redox conditions at Jianghan Plain of Central China. Science of the Total Environment, 2017, 607-608, 992-1000.	8.0	56
64	Shifts in pore connectivity from precipitation versus groundwater rewetting increases soil carbon loss after drought. Nature Communications, 2017, 8, 1335.	12.8	88
65	What can we learn from in-soil imaging of a live plant: X-ray Computed Tomography and 3D numerical simulation of root-soil system. Rhizosphere, 2017, 3, 259-262.	3.0	12
66	Multiscale Investigation on Biofilm Distribution and Its Impact on Macroscopic Biogeochemical Reaction Rates. Water Resources Research, 2017, 53, 8698-8714.	4.2	26
67	Regulation-Structured Dynamic Metabolic Model Provides a Potential Mechanism for Delayed Enzyme Response in Denitrification Process. Frontiers in Microbiology, 2017, 8, 1866.	3.5	40
68	Soil Respiration and Bacterial Structure and Function after 17 Years of a Reciprocal Soil Transplant Experiment. PLoS ONE, 2016, 11, e0150599.	2.5	60
69	Characteristics and Kinetic Analysis of AQS Transformation and Microbial Goethite Reduction:Insight into "Redox mediator-Microbe-Iron oxide―Interaction Process. Scientific Reports, 2016, 6, 23718.	3.3	3
70	Pore-scale investigation on the response of heterotrophic respiration to moisture conditions in heterogeneous soils. Biogeochemistry, 2016, 131, 121-134.	3.5	54
71	In situ Fe-sulfide coating for arsenic removal under reducing conditions. Journal of Hydrology, 2016, 534, 42-49.	5.4	29
72	Grain-Size Based Additivity Models for Scaling Multi-rate Uranyl Surface Complexation in Subsurface Sediments. Mathematical Geosciences, 2016, 48, 511-535.	2.4	11

#	Article	IF	CITATIONS
73	Internal Domains of Natural Porous Media Revealed: Critical Locations for Transport, Storage, and Chemical Reaction. Environmental Science & Technology, 2016, 50, 2811-2829.	10.0	76
74	Nitrate bioreduction in redox-variable low permeability sediments. Science of the Total Environment, 2016, 539, 185-195.	8.0	32
75	In-situ arsenic remediation by aquifer iron coating: Field trial in the Datong basin, China. Journal of Hazardous Materials, 2016, 302, 19-26.	12.4	15
76	6. Pore-Scale Process Coupling and Effective Surface Reaction Rates in Heterogeneous Subsurface Materials. , 2015, , 191-216.		1
77	A Fluorescence-Based Method for Rapid and Direct Determination of Polybrominated Diphenyl Ethers in Water. Journal of Analytical Methods in Chemistry, 2015, 2015, 1-10.	1.6	5
78	In situ treatment of arsenic contaminated groundwater by aquifer iron coating: Experimental study. Science of the Total Environment, 2015, 527-528, 38-46.	8.0	24
79	Pore and continuum scale study of the effect of subgrid transport heterogeneity on redox reaction rates. Geochimica Et Cosmochimica Acta, 2015, 163, 140-155.	3.9	16
80	Release and control of hydrogen sulfide during sludge thermal drying. Journal of Hazardous Materials, 2015, 296, 61-67.	12.4	25
81	Pore-Scale Process Coupling and Effective Surface Reaction Rates in Heterogeneous Subsurface Materials. Reviews in Mineralogy and Geochemistry, 2015, 80, 191-216.	4.8	31
82	⁹⁹ Tc(VII) Retardation, Reduction, and Redox Rate Scaling in Naturally Reduced Sediments. Environmental Science & Technology, 2015, 49, 13403-13412.	10.0	15
83	Dynamic Metabolic Modeling of Denitrifying Bacterial Growth: The Cybernetic Approach. Industrial & Engineering Chemistry Research, 2015, 54, 10221-10227.	3.7	32
84	Comparison of 20 nm silver nanoparticles synthesized with and without a gold core: Structure, dissolution in cell culture media, and biological impact on macrophages. Biointerphases, 2015, 10, 031003.	1.6	27
85	Simulations of ecosystem hydrological processes using a unified multi-scale model. Ecological Modelling, 2015, 296, 93-101.	2.5	10
86	Impact of sedimentary provenance and weathering on arsenic distribution in aquifers of the Datong basin, China: Constraints from elemental geochemistry. Journal of Hydrology, 2014, 519, 3541-3549.	5.4	36
87	Uranium(VI) reduction by nanoscale zero-valent iron in anoxic batch systems: The role of Fe(II) and Fe(III). Chemosphere, 2014, 117, 625-630.	8.2	28
88	Steady state estimation of soil organic carbon using satelliteâ€derived canopy leaf area index. Journal of Advances in Modeling Earth Systems, 2014, 6, 1049-1064.	3.8	6
89	Transformation of heavy metal speciation during sludge drying: Mechanistic insights. Journal of Hazardous Materials, 2014, 265, 96-103.	12.4	68
90	Molecular Dynamics Simulations of Uranyl and Uranyl Carbonate Adsorption at Aluminosilicate Surfaces. Environmental Science & Technology, 2014, 48, 3899-3907.	10.0	65

#	Article	IF	CITATIONS
91	Effect of Subgrid Heterogeneity on Scaling Geochemical and Biogeochemical Reactions: A Case of U(VI) Desorption. Environmental Science & Technology, 2014, 48, 1745-1752.	10.0	34
92	Long-term kinetics of uranyl desorption from sediments under advective conditions. Water Resources Research, 2014, 50, 855-870.	4.2	14
93	Uncertainty analysis of multi-rate kinetics of uranium desorption from sediments. Journal of Contaminant Hydrology, 2014, 156, 1-15.	3.3	12
94	Investigation of U(VI) Adsorption in Quartz–Chlorite Mineral Mixtures. Environmental Science & Technology, 2014, 48, 7766-7773.	10.0	16
95	Transport of fluorescently labeled hydroxyapatite nanoparticles in saturated granular media at environmentally relevant concentrations of surfactants. Colloids and Surfaces A: Physicochemical and Engineering Aspects, 2014, 457, 58-66.	4.7	34
96	Influence of calcite on uranium(VI) reactive transport in the groundwater–river mixing zone. Journal of Contaminant Hydrology, 2014, 156, 27-37.	3.3	29
97	A Unified Multiscale Model for Pore-ScaleFlow Simulations in Soils. Soil Science Society of America Journal, 2014, 78, 108-118.	2.2	23
98	Assessment of controlling processes for field-scale uranium reactive transport under highly transient flow conditions. Water Resources Research, 2014, 50, 1006-1024.	4.2	22
99	Persistence of uranium groundwater plumes: Contrasting mechanisms at two DOE sites in the groundwater–river interaction zone. Journal of Contaminant Hydrology, 2013, 147, 45-72.	3.3	136
100	Structure, Kinetics, and Thermodynamics of the Aqueous Uranyl(VI) Cation. Journal of Physical Chemistry A, 2013, 117, 6421-6432.	2.5	52
101	Scale-dependent rates of uranyl surface complexation reaction in sediments. Geochimica Et Cosmochimica Acta, 2013, 105, 326-341.	3.9	54
102	Fe _{3–<i>x</i>} Ti _{<i>x</i>} O ₄ Nanoparticles as Tunable Probes of Microbial Metal Oxidation. Journal of the American Chemical Society, 2013, 135, 8896-8907.	13.7	43
103	Transport and retention of engineered nanoporous particles in porous media: Effects of concentration and flow dynamics. Colloids and Surfaces A: Physicochemical and Engineering Aspects, 2013, 417, 89-98.	4.7	30
104	Micromodel Investigation of Transport Effect on the Kinetics of Reductive Dissolution of Hematite. Environmental Science & Technology, 2013, 47, 4131-4139.	10.0	14
105	Characterizing particleâ€scale equilibrium adsorption and kinetics of uranium(VI) desorption from Uâ€contaminated sediments. Water Resources Research, 2013, 49, 1163-1177.	4.2	27
106	Diffusion and Adsorption of Uranyl Carbonate Species in Nanosized Mineral Fractures. Environmental Science & Technology, 2012, 46, 1632-1640.	10.0	55
107	Fluorescent Functionalized Mesoporous Silica for Radioactive Material Extraction. Separation Science and Technology, 2012, 47, 1507-1513.	2.5	11
108	Quantitative 3-D Elemental Mapping by LA-ICP-MS of a Basaltic Clast from the Hanford 300 Area, Washington, USA. Environmental Science & Technology, 2012, 46, 2025-2032.	10.0	36

#	Article	IF	CITATIONS
109	Modeling intragranular diffusion in lowâ€connectivity granular media. Water Resources Research, 2012, 48, .	4.2	11
110	Identification and Characterization of MtoA: A Decaheme c-Type Cytochrome of the Neutrophilic Fe(II)-Oxidizing Bacterium Sideroxydans lithotrophicus ES-1. Frontiers in Microbiology, 2012, 3, 37.	3.5	186
111	Effect of Grain Size on Uranium(VI) Surface Complexation Kinetics and Adsorption Additivity. Environmental Science & Technology, 2011, 45, 6025-6031.	10.0	60
112	Simulating adsorption of U(VI) under transient groundwater flow and hydrochemistry: Physical versus chemical nonequilibrium model. Water Resources Research, 2011, 47, .	4.2	16
113	Multispecies diffusion models: A study of uranyl species diffusion. Water Resources Research, 2011, 47,	4.2	43
114	Bioreduction of Fe-bearing clay minerals and their reactivity toward pertechnetate (Tc-99). Geochimica Et Cosmochimica Acta, 2011, 75, 5229-5246.	3.9	128
115	Uranium(VI) diffusion in low-permeability subsurface materials. Radiochimica Acta, 2010, 98, 719-726.	1.2	7
116	Resupply mechanism to a contaminated aquifer: A laboratory study of U(VI) desorption from capillary fringe sediments. Geochimica Et Cosmochimica Acta, 2010, 74, 5155-5170.	3.9	24
117	Molecular simulation of the diffusion of uranyl carbonate species in aqueous solution. Geochimica Et Cosmochimica Acta, 2010, 74, 4937-4952.	3.9	109
118	Scale dependence of intragranular porosity, tortuosity, and diffusivity. Water Resources Research, 2010, 46, .	4.2	30
119	In-Situ Measurements of Engineered Nanoporous Particle Transport in Saturated Porous Media. Environmental Science & Technology, 2010, 44, 8190-8195.	10.0	25
120	Uranium(VI) Removal by Nanoscale Zerovalent Iron in Anoxic Batch Systems. Environmental Science & Technology, 2010, 44, 7783-7789.	10.0	140
121	Pathways of Aqueous Cr(VI) Attenuation in a Slightly Alkaline Oxic Subsurface. Environmental Science & Technology, 2009, 43, 1071-1077.	10.0	23
122	Microbial Reduction of Intragrain U(VI) in Contaminated Sediment. Environmental Science & Technology, 2009, 43, 4928-4933.	10.0	24
123	Inhibition Effect of Secondary Phosphate Mineral Precipitation on Uranium Release from Contaminated Sediments. Environmental Science & Technology, 2009, 43, 8344-8349.	10.0	30
124	Study of Sorption-Retarded U(VI) Diffusion in Hanford Silt/Clay Material. Environmental Science & Technology, 2009, 43, 7706-7711.	10.0	23
125	Reduction and long-term immobilization of technetium by Fe(II) associated with clay mineral nontronite. Chemical Geology, 2009, 264, 127-138.	3.3	108
126	Physical control on CCl4 and CHCl3 desorption from artificially contaminated and aged sediments with supercritical carbon dioxide. Chemosphere, 2009, 74, 494-500.	8.2	3

#	Article	IF	CITATIONS
127	Oxidative dissolution potential of biogenic and abiogenic TcO2 in subsurface sediments. Geochimica Et Cosmochimica Acta, 2009, 73, 2299-2313.	3.9	54
128	Molecular Simulations of Water and Ion Diffusion in Nanosized Mineral Fractures. Environmental Science & Technology, 2009, 43, 777-782.	10.0	135
129	Kinetics of Uranium(VI) Desorption from Contaminated Sediments: Effect of Geochemical Conditions and Model Evaluation. Environmental Science & Technology, 2009, 43, 6560-6566.	10.0	89
130	Hydrogenase―and outer membrane <i>c</i> â€type cytochromeâ€facilitated reduction of technetium(VII) by <i>Shewanella oneidensis</i> MRâ€1. Environmental Microbiology, 2008, 10, 125-136.	3.8	74
131	Scaleâ€dependent desorption of uranium from contaminated subsurface sediments. Water Resources Research, 2008, 44, .	4.2	123
132	Molecular dynamics simulations of the orthoclase (001)- and (010)-water interfaces. Geochimica Et Cosmochimica Acta, 2008, 72, 1481-1497.	3.9	68
133	Fe2+ sorption onto nontronite (NAu-2). Geochimica Et Cosmochimica Acta, 2008, 72, 5361-5371.	3.9	50
134	Advective Removal of Intraparticle Uranium from Contaminated Vadose Zone Sediments, Hanford, U.S Environmental Science & Technology, 2008, 42, 1565-1571.	10.0	30
135	Kinetics of Reduction of Fe(III) Complexes by Outer Membrane Cytochromes MtrC and OmcA of <i>Shewanella oneidensis</i> MR-1. Applied and Environmental Microbiology, 2008, 74, 6746-6755.	3.1	89
136	A cryogenic fluorescence spectroscopic study of uranyl carbonate, phosphate and oxyhydroxide minerals. Radiochimica Acta, 2008, 96, 591-598.	1.2	51
137	A spectroscopic study of the effect of ligand complexation on the reduction of uranium(VI) by anthraquinone-2,6-disulfonate (AH ₂ DS). Radiochimica Acta, 2008, 96, 599-605.	1.2	6
138	Reduction of pertechnetate [Tc(VII)] by aqueous Fe(II) and the nature of solid phase redox products. Geochimica Et Cosmochimica Acta, 2007, 71, 2137-2157.	3.9	154
139	Influence of biogenic Fe(II) on the extent of microbial reduction of Fe(III) in clay minerals nontronite, illite, and chlorite. Geochimica Et Cosmochimica Acta, 2007, 71, 1145-1158.	3.9	137
140	Kinetics of Reductive Dissolution of Hematite by Bioreduced Anthraquinone-2,6-disulfonate. Environmental Science & Technology, 2007, 41, 7730-7735.	10.0	80
141	Cr(VI) Removal from Aqueous Solution by Activated Carbon Coated with Quaternized Poly(4-vinylpyridine). Environmental Science & Technology, 2007, 41, 4748-4753.	10.0	185
142	Kinetic Analysis of Microbial Reduction of Fe(III) in Nontronite. Environmental Science & Technology, 2007, 41, 2437-2444.	10.0	41
143	An Ion Diffusion Model in Semi-Permeable Clay Materials. Environmental Science & Technology, 2007, 41, 5403-5409.	10.0	15
144	Influence of calcium on microbial reduction of solid phase uranium(VI). Biotechnology and Bioengineering, 2007, 97, 1415-1422.	3.3	22

#	Article	IF	CITATIONS
145	Reduction of Uranyl in the Interlayer Region of Low Iron Micas under Anoxic and Aerobic Conditions. Environmental Science & Technology, 2006, 40, 5003-5009.	10.0	45
146	Microscopic reactive diffusion of uranium in the contaminated sediments at Hanford, United States. Water Resources Research, 2006, 42, .	4.2	49
147	Kinetics of Microbial Reduction of Solid Phase U(VI). Environmental Science & Technology, 2006, 40, 6290-6296.	10.0	25
148	Microscale controls on the fate of contaminant uranium in the vadose zone, Hanford Site, Washington. Geochimica Et Cosmochimica Acta, 2006, 70, 1873-1887.	3.9	82
149	The dissolution of synthetic Na-boltwoodite in sodium carbonate solutions. Geochimica Et Cosmochimica Acta, 2006, 70, 4836-4849.	3.9	30
150	Oxidative Remobilization of Biogenic Uranium(IV) Precipitates. Journal of Environmental Quality, 2005, 34, 1763-1771.	2.0	59
151	Kinetic Desorption and Sorption of U(VI) during Reactive Transport in a Contaminated Hanford Sediment. Environmental Science & Technology, 2005, 39, 3157-3165.	10.0	137
152	Influence of Sediment Bioreduction and Reoxidation on Uranium Sorption. Environmental Science & Technology, 2005, 39, 4125-4133.	10.0	30
153	Fluorescence spectroscopy of U(VI)-silicates and U(VI)-contaminated Hanford sediment. Geochimica Et Cosmochimica Acta, 2005, 69, 1391-1403.	3.9	136
154	Influence of Calcite and Dissolved Calcium on Uranium(VI) Sorption to a Hanford Subsurface Sediment. Environmental Science & Technology, 2005, 39, 7949-7955.	10.0	137
155	A cation exchange model to describe Cs+ sorption at high ionic strength in subsurface sediments at Hanford site, USA. Journal of Contaminant Hydrology, 2004, 68, 217-238.	3.3	60
156	An electrodynamics-based model for ion diffusion in microbial polysaccharides. Colloids and Surfaces B: Biointerfaces, 2004, 38, 55-65.	5.0	13
157	Reduction of TcO4â^' by sediment-associated biogenic Fe(II). Geochimica Et Cosmochimica Acta, 2004, 68, 3171-3187.	3.9	184
158	Dissolution of uranyl microprecipitates in subsurface sediments at Hanford Site, USA. Geochimica Et Cosmochimica Acta, 2004, 68, 4519-4537.	3.9	110
159	Cryogenic Laser Induced Fluorescence Characterization of U(VI) in Hanford Vadose Zone Pore Waters. Environmental Science & Technology, 2004, 38, 5591-5597.	10.0	164
160	Influence of electron donor/acceptor concentrations on hydrous ferric oxide (HFO) bioreduction. Biodegradation, 2003, 14, 91-103.	3.0	69
161	Effect of Temperature on Cs+Sorption and Desorption in Subsurface Sediments at the Hanford Site, U.S.A Environmental Science & Technology, 2003, 37, 2640-2645.	10.0	66
162	Supercritical Fluid Extraction of Toxic Heavy Metals and Uranium from Acidic Solutions with Sulfur-Containing Organophosphorus Reagents. Industrial & Engineering Chemistry Research, 2003, 42, 1400-1405.	3.7	42

#	Article	IF	CITATIONS
163	Desorption kinetics of radiocesium from subsurface sediments at Hanford Site, USA. Geochimica Et Cosmochimica Acta, 2003, 67, 2893-2912.	3.9	120
164	Modeling the Inhibition of the Bacterial Reduction of U(VI) by β-MnO2(s). Environmental Science & Technology, 2002, 36, 1452-1459.	10.0	67
165	Sorption of Cs+ to micaceous subsurface sediments from the Hanford site, USA. Geochimica Et Cosmochimica Acta, 2002, 66, 193-211.	3.9	298
166	Influence of Mn oxides on the reduction of uranium(VI) by the metal-reducing bacterium Shewanella putrefaciens. Geochimica Et Cosmochimica Acta, 2002, 66, 3247-3262.	3.9	170
167	Reduction kinetics of Fe(III), Co(III), U(VI), Cr(VI), and Tc(VII) in cultures of dissimilatory metal-reducing bacteria. Biotechnology and Bioengineering, 2002, 80, 637-649.	3.3	293
168	Back Diffusion of Chlorinated Solvent Contaminants from a Natural Aquitard to a Remediated Aquifer Under Well-Controlled Field Conditions: Predictions and Measurements. Ground Water, 2002, 40, 175-184.	1.3	126
169	Diffusion-Limited Contamination and Decontamination in a Layered Aquitard: Forensic and Predictive Analysis of Field Data. The IMA Volumes in Mathematics and Its Applications, 2002, , 179-194.	0.5	0
170	Microbial Reduction of Fe(III) and Sorption/Precipitation of Fe(II) onShewanella putrefaciensStrain CN32. Environmental Science & amp; Technology, 2001, 35, 1385-1393.	10.0	136
171	Dissimilatory bacterial reduction of Al-substituted goethite in subsurface sediments. Geochimica Et Cosmochimica Acta, 2001, 65, 2913-2924.	3.9	98
172	Uncertainties of Monod Kinetic Parameters Nonlinearly Estimated from Batch Experiments. Environmental Science & Technology, 2001, 35, 133-141.	10.0	72
173	Kinetic Analysis of the Bacterial Reduction of Goethite. Environmental Science & Technology, 2001, 35, 2482-2490.	10.0	199
174	Use of the generalized integral transform method for solving equations of solute transport in porous media. Advances in Water Resources, 2000, 23, 483-492.	3.8	60
175	Application of inverse methods to contaminant source identification from aquitard diffusion profiles at Dover AFB, Delaware. Water Resources Research, 1999, 35, 1975-1985.	4.2	98
176	Title is missing!. Transport in Porous Media, 1998, 30, 25-43.	2.6	54
177	Pore water geochemistry near the sediment-water interface of a zoned, freshwater wetland in the southeastern United States. Environmental Geology, 1998, 33, 143-153.	1.2	32
178	Analytical modeling of diffusion-limited contamination and decontamination in a two-layer porous medium. Advances in Water Resources, 1998, 21, 297-313.	3.8	65
179	A diffusion-based interpretation of tetrachloroethene and trichloroethene concentration profiles in a groundwater aquitard. Water Resources Research, 1997, 33, 2741-2757.	4.2	83